

Experimental Observation of a Radiative Wave Generated in Xenon by a Laser-Driven Supercritical Shock

J. C. Bozier, G. Thiell, J. P. Le Breton, S. Azra, M. Decroisette, and D. Schirmann

Commissariat à l'Energie Atomique, Centre d'Etudes de Limeil-Valenton, 94190 Villeneuve-Saint-Georges, France

(Received 24 February 1986)

First experimental evidence of a radiative wave propagating ahead of a supercritical shock is given. An aluminum piston driven by laser light at wavelengths of 1.06 and 0.35 μm induces the shock wave in xenon gas. The plane piston velocity ranges from 2.5×10^6 to 1.2×10^7 $\text{cm} \cdot \text{s}^{-1}$ and the gas pressure is up to 6 bars. Experimental results are in good agreement with a simple analytical model of the propagation of a radiative wave in front of a supercritical shock wave when the approximation of radiation heat conduction is assumed.

PACS numbers: 52.35.Tc, 44.40.+a, 51.70.+f, 52.50.Jm

Radiative phenomena occurring in shock waves were observed in strong explosions in air and described many years ago.^{1,2} The structure and the luminosity of strong shock waves in gases have been theoretically investigated,¹ taking radiation into account. However, experimental results in this field of physics on laboratory plasmas are very scarce. Optical precursors have been observed in explosive-driven shock tubes³ and in magnetically driven shock-wave boxes⁴ but the characteristic shock velocities for such systems are less than 4×10^6 $\text{cm} \cdot \text{s}^{-1}$. More recently, blast-wave experiments studied in an ambient gas fill surrounding a Nd-laser-irradiated target have revealed deviations of the shock profile from the ideal one, attributed to photoionization effects.⁵

A high-power laser is a well adapted tool to achieve high pressures in thin plane targets^{6,7} which may act as a piston.⁸ Shorter wavelengths (0.35 μm) present the advantages of higher hydrodynamic efficiency⁷ and smaller number of hot electrons.⁹

In this Letter, it is experimentally evidenced that a radiative wave propagates ahead of a strong shock induced by a laser-accelerated plane piston moving into xenon gas with a constant and sufficiently high velocity. The analysis of the experimental results is based on an analytic model of the propagation of a radiative wave in front of a supercritical shock wave when the radiation heat conduction approximation is assumed.

Within an adiabatic approximation the internal energy per unit mass of the gas $U_p^2/2$, where U_p is the velocity of the piston, is related to the shock temperature T_C by

$$T_C = U_p^2/2C_V, \quad (1)$$

where C_V is the specific heat. In the experiments presented here, we choose xenon gas for which $C_V = 1.85 \times 10^7$ $\text{erg} \cdot \text{g}^{-1} \cdot \text{K}^{-1}$. The piston velocity ranges from 5×10^6 to 1.2×10^7 $\text{cm} \cdot \text{s}^{-1}$ and consequently the shock is supercritical.¹ It is losing energy through radiation. Its temperature ranges from lower

than T_C up to 3×10^5 K. In this range of temperature, the variation of C_V is about a factor of 2. The above value of C_V is an averaged value. Note that the radiative wave temperature T varies as $1/C_V^{1/7.2}$ as can be deduced from Eqs. (2), (3), and (5). Hence, T depends weakly on C_V .

Assuming that the radiation heat conduction approximation is valid, we get the equations¹

$$\partial T/\partial t = - (1/\rho_0 C_V) \nabla \cdot \mathbf{S}_{\text{rad}} \quad (2)$$

and

$$S_{\text{rad}} = \frac{16}{3} \lambda \sigma T^3 dT/dx, \quad (3)$$

where S_{rad} is the radiation flux, dT/dx the temperature gradient in the radiation heat conduction layer ahead of the shock front, σ the Stefan-Boltzmann constant, and λ the Rosseland mean free path. λ can be written as proportional to some power of the temperature T and density ρ_0 of the gas; for xenon gas¹⁰

$$\lambda = 2.3 \times 10^{-17} \frac{[T/(1 \text{ K})]^{2.2}}{[\rho_0/(1 \text{ g} \cdot \text{cm}^{-3})]^{1.2}} \text{ cm}. \quad (4)$$

The geometrical location x_{rf} of the radiative wave front is then determined by a dimensional analysis with the following simplifying assumptions: (a) The piston is of finite plane geometry; (b) the radiation heat conduction approximation applies, i.e., $\lambda \ll L$, where L is the characteristic length of the experimental system; (c) the piston moves into the gas with a constant velocity; and (d) the piston is considered as a constant radiation flux source at rest. The validity of this last hypothesis is supported by the fact that the radiation flux through the mass of the compressed gas is nearly the same as it would be through an equal mass of gas at ρ_0 because the specific heat C_V and the optical thickness of the gas are weakly dependent on density.

After some calculations, x_{rf} is given from Eqs.

(1)–(4) as a function of time:

$$\rho_0 x_{\text{rf}} \approx (1.3 \times 10^{-16} \sigma)^{1/7.2} (U_p^3/2)^{5.2/7.2} \rho_0^{5/7.2} (t/C_V)^{6.2/7.2}. \quad (5)$$

The laws describing the radiation and electronic heat conduction processes are identical.¹ A similar analytical model for electrons gives in the same way an expression for the geometrical location of the electronic wave front:

$$\rho_0 x_{\text{ef}} \approx (10^{-6})^{2/9} (U_p^3/2)^{5/9} \rho_0^{7/9} (t/C_V)^{7/9}. \quad (6)$$

The results of both calculations, compared in Fig. 1 for $\rho_0 = 10^{-2} \text{ g} \cdot \text{cm}^{-3}$ and $U_p = 5 \times 10^6 \text{ cm} \cdot \text{s}^{-1}$, show that the electronic heat conduction wave remains closely ahead of the shock wave while the radiative wave rapidly breaks away.

Experimentally, high piston velocities can be achieved with thin aluminum foils irradiated at high irradiances in the range from 2×10^{14} to $5 \times 10^{14} \text{ W} \cdot \text{cm}^{-2}$. A Nd-glass laser delivering a 1-nsec, 40-J pulse or a 1-nsec frequency-tripled laser pulse with energies up to 17 J is used. In each case, the focal spot diameter (FWHM) is about $100 \mu\text{m}$ ($\pm 20 \mu\text{m}$). Lateral diffusion of energy is known to reduce the non-uniformities¹¹ and to yield a plane acceleration of the piston.¹² In these conditions, sufficiently high velocities are attained with $10\text{-}\mu\text{m}$ -thick aluminum foils: from 5×10^6 to $8 \times 10^6 \text{ cm} \cdot \text{s}^{-1}$ and slightly greater than $10^7 \text{ cm} \cdot \text{s}^{-1}$, respectively, for 1.06- and $0.35\text{-}\mu\text{m}$ laser wavelengths.¹²

To study the propagation of the thermal wave in a nearly plane situation, we use a kind of miniature shock tube which consists of a 1-cm-long tube of square cross section ($200 \times 200 \mu\text{m}^2$). This value is chosen by taking into account the above hypothesis (b) and Eq. (4). The quartz walls of the tube have surfaces of optical quality and permit transverse observation of the propagation of the luminous phenomena along the tube. One of the extremities is closed with a

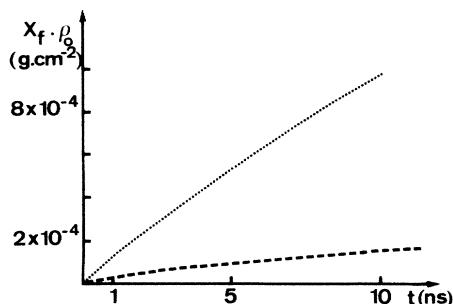


FIG. 1. Evolution diagram of the front of both the radiative wave (dotted line) and the electronic wave (dashed line) in $10^{-2}\text{-g} \cdot \text{cm}^{-3}$ xenon gas, for a constant piston velocity of $5 \times 10^6 \text{ cm} \cdot \text{s}^{-1}$.

$10\text{-}\mu\text{m}$ -thick aluminum piston on which the laser beam is focused with a $f/6.7$, 600-mm-focal-length lens. The focusing accuracy of laser energy on the center of the piston is insured to be about $50 \mu\text{m}$. At the other end, the shock tube is filled with gas by means of a feeder tube the tip of which is situated at $750 \mu\text{m}$ from the piston's initial position and is gilded so that it constitutes an obstacle with a high Z number.

The evolutions of all luminous regions which appear inside the shock tube after laser irradiation of the Al piston are recorded by means of a streak camera. The slit of the camera is parallel to the axis of the shock tube so that the propagation of the piston and the thermal front inside the shock tube, as well as the time at which the obstacle glows, can be recorded.

Laser irradiances beyond $2 \times 10^{14} \text{ W} \cdot \text{cm}^{-2}$ induce a strong shock wave in the Al piston.⁶ At the time of emergence of such a shock wave from the rear-side free surface, the piston begins to move into the gas. It generates a strong shock wave in the gas and a thermal front propagating ahead of it. The thinness of the shock does not permit one to distinguish the luminosity of the compressed gas from the luminosity of the unloading piston. In these experiments, the energy of the piston is very high compared to the energy transferred from the piston to the gas. Consequently, the slowing down of the piston is negligible. Once it is reached by the thermal front, the high- Z obstacle is heated and becomes luminous before being reached by the shock wave. The distance between the piston and the radiation wave front is not very different ($\leq 300 \mu\text{m}$ in Figs. 2 and 3) from the shock tube cross section, and so the radiation losses to the walls are low.

Figure 2 shows that in vacuum, a luminous front moves along the shock tube with a nearly constant velocity of $(5 \pm 1) \times 10^6 \text{ cm} \cdot \text{s}^{-1}$ [Fig. 2(a)]. It corresponds to the motion of the Al piston after irradiation with the $1.06\text{-}\mu\text{m}$ laser pulse at an irradiance of $(4 \pm 1) \times 10^{14} \text{ W} \cdot \text{cm}^{-2}$. When the shock tube is filled with xenon gas, two additional effects can be observed in Figs. 2(b) and 2(c).

(i) A luminous front moves ahead of the piston with a velocity slightly greater than $10^7 \text{ cm} \cdot \text{s}^{-1}$. Taking into account the value of this velocity and the theoretical diagram of Fig. 1, this luminous front corresponds to the propagation of a radiative wave in xenon gas.

(ii) The obstacle becomes luminous just at the time it is reached by the thermal front. The distance of $750 \mu\text{m}$ from the piston to the obstacle corresponds to a few Rosseland mean free paths. The comparison of Figs. 2(b) and 2(c) shows that if the gas pressure is increased from 2 bars ($\rho_0 = 10^{-2} \text{ g} \cdot \text{cm}^{-3}$) to 6 bars, the

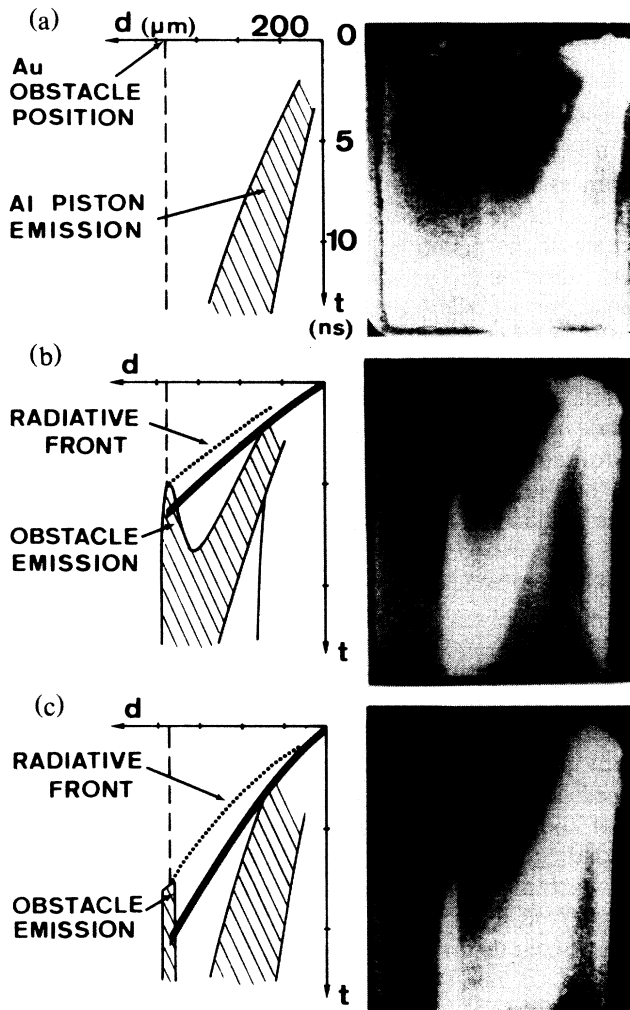


FIG. 2. Comparison between the streak photographs (hatched zones) and the results of the radiative heat conduction model (solid lines). Dotted lines represent the experimental radiative front. The $10\text{-}\mu\text{m}$ -thick Al piston moves in (a) vacuum, (b) 2 bars of xenon gas, and (c) 6 bars of xenon gas. The laser is incident from the right and the irradiance is about $4 \times 10^{14} \text{ W} \cdot \text{cm}^{-2}$.

radiative front velocity is decreased by a factor of 1.4, while the piston velocity is unchanged. These observations are in good agreement with the theoretical predictions of Eq. (5).

In Fig. 3, the experimental results obtained with three different piston velocities, 2.5×10^6 , 5×10^6 , and $1.2 \times 10^7 \text{ cm} \cdot \text{s}^{-1}$, show first that for the lowest velocity [Fig. 3(a)] the radiative front does not loom up out of the luminosity of the piston in accordance with the model, and then that if the piston velocity is increased by a factor of 2.4 [Figs. 3(b) and 3(c)] the obstacle glows simultaneously with the beginning of the piston movement. This last result is qualitatively in agree-

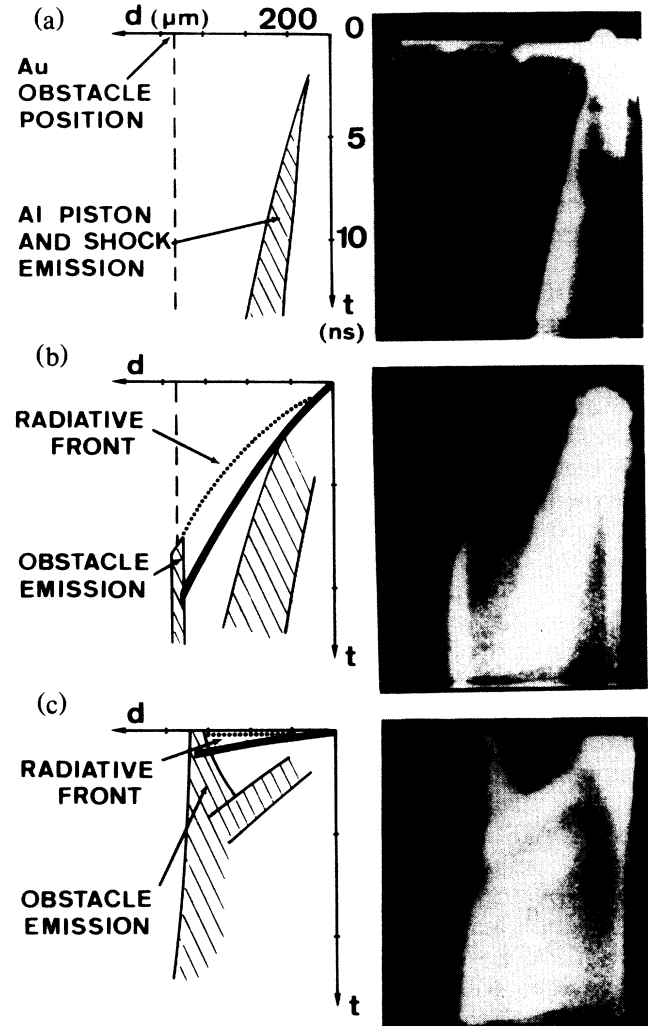


FIG. 3. Streak photographs compared to radiation-model results obtained for three different piston velocities in a shock tube filled with 6 bars of xenon. (a), (b) 2.5×10^6 and $5 \times 10^6 \text{ cm} \cdot \text{s}^{-1}$, respectively, with $1.06\text{-}\mu\text{m}$ laser light; (c) $1.2 \times 10^7 \text{ cm} \cdot \text{s}^{-1}$ with $0.35\text{-}\mu\text{m}$ laser light.

ment with the theoretical scaling law (5), the radiative front velocity being expected to be multiplied by 6.7 when the piston velocity is multiplied by 2.4. Accordingly, the obstacle must glow about 1 nsec after the beginning of the movement of the piston. A possible explanation could be that in $0.35\text{-}\mu\text{m}$ experiments [Fig. 3(b)] the gas temperature is high enough to induce a radiation regime out of equilibrium. And, because of the transparency of the gas for the photons born in the shock wave, the obstacle is heated quite early.

It has still to be noticed that the hot electron temperature created by resonant absorption is about 6 keV for $5 \times 10^{14} \text{ W} \cdot \text{cm}^{-2}$ irradiance at $1.06\text{-}\mu\text{m}$ laser wavelength.¹³ The stopping range of these electrons is

about $1\ \mu\text{m}$ in Al. In $0.35\text{-}\mu\text{m}$ experiments the flux of suprathermal electrons is greatly reduced.⁹ When the experiments are done in vacuum, even at the highest irradiance the obstacle does not become luminous. Therefore, a $10\text{-}\mu\text{m}$ -thick Al foil prevents the obstacle from being preheated by suprathermal electrons¹⁴ or x rays emitted from the piston^{15,16} [Fig. 2(a)].

The luminous front moving ahead of the piston and the brightness of the obstacle are really two effects which only appear when the shock tube is filled with gas. Laser energy was relatively low ($\leq 40\ \text{J}$) in our experiments so that the shock temperature is about a few tens of electron volts. However, the radiant flux is high enough to induce a significant expansion of the Au obstacle, especially in $0.35\text{-}\mu\text{m}$ experiments [Figs. 2(b) and 3(c)]. These experimental results are in good agreement with the analytic model of radiative wave propagation. Accordingly, the electronic heat conduction¹⁷ does not take a major part in the interpretation of our experimental results.

In this Letter, it is experimentally evidenced that a radiation thermal wave propagates ahead of a supercritical shock wave driven by laser light in xenon gas. Future interpretation will deal with more detailed parametric studies such as the nature of the gas (xenon, argon, air, . . .), i.e., the heat capacity C_V , and correlatively the piston velocity.

We would like to thank many people associated with these experiments. In particular, we are greatly indebted to J. Lauriou for operating the laser and Ph. Eyharts for target fabrication.

¹Ya. B. Zel'dovich and Yu. P. Raizer, in *Physics of Shock Waves and High Temperature Hydrodynamic Phenomena*, edited by W. D. Hayes and R. F. Probstein (Academic, New

York, 1966).

²Yu. P. Raizer, Zh. Eksp. Teor. Fiz. **33**, 101 (1958) [Sov. Phys. JETP **6**, 77 (1958)].

³R. E. Duff and F. I. Peterson, J. Appl. Phys. **51**, 3957 (1980).

⁴J. W. Shearer, J. W. Beasley, A. Reyenga, and D. Steinberg, in *Megagauss Physics and Technology*, edited by P. J. Turchi (Plenum, New York, 1980).

⁵B. H. Ripin, J. A. Stamper, E. A. McLean, A. N. Mostovych, J. Grun, C. K. Manka, and S. T. Kacendar, Bull. Am. Phys. Soc. **29**, 1177 (1984).

⁶F. Cottet, J. P. Romain, R. Fabbro, and B. Faral, Phys. Rev. Lett. **52**, 1884 (1984).

⁷B. Meyer and G. Thiell, Phys. Fluids **27**, 302 (1984).

⁸S. P. Obenshain, R. R. Whitlock, E. A. McLean, B. H. Ripin, R. H. Price, D. W. Phillion, E. M. Campbell, M. D. Rosen, and J. M. Auerbach, Phys. Rev. Lett. **50**, 44 (1983).

⁹B. Yaakobi, T. Boehly, P. Bourke, Y. Conturie, R. S. Craxton, J. Delettrez, J. M. Forsyth, R. D. Frankel, L. M. Goldman, R. L. McCrory, M. C. Richardson, W. Seka, D. Shvarts, and J. M. Soures, Opt. Commun. **39**, 175 (1981).

¹⁰W. F. Huebner, of Los Alamos Science Liaison Co., 253 Rio Bravo, Los Alamos, NM 87544, has provided us with unpublished opacity calculations for xenon.

¹¹J. H. Gardner and S. E. Bodner, Phys. Rev. Lett. **47**, 1137 (1981); S. E. Bodner, J. Fusion Energy **1**, 221 (1981).

¹²G. Thiell, B. Meyer, P. Aussage, and X. Fortin, Opt. Commun. **46**, 305 (1983).

¹³D. G. Colombant and W. M. Manheimer, J. Appl. Phys. **51**, 6120 (1980).

¹⁴B. Meyer, G. Morin, and G. Thiell, J. Appl. Phys. **53**, 2947 (1982).

¹⁵J. Mizui, N. Yamaguchi, S. Takagi, and K. Nishihara, Phys. Rev. Lett. **47**, 1000 (1981).

¹⁶J. L. Bocher, M. Decroisette, P. A. Holstein, M. Louis-Jacquet, B. Meyer, A. Saleres, and G. Thiell, Phys. Rev. Lett. **52**, 823 (1984).

¹⁷N. N. Zorev, G. Y. Sklizkov, and A. S. Shikanov, Pis'ma Zh. Eksp. Teor. Fiz. **31**, 610 (1980) [JETP Lett. **31**, 574 (1980)].

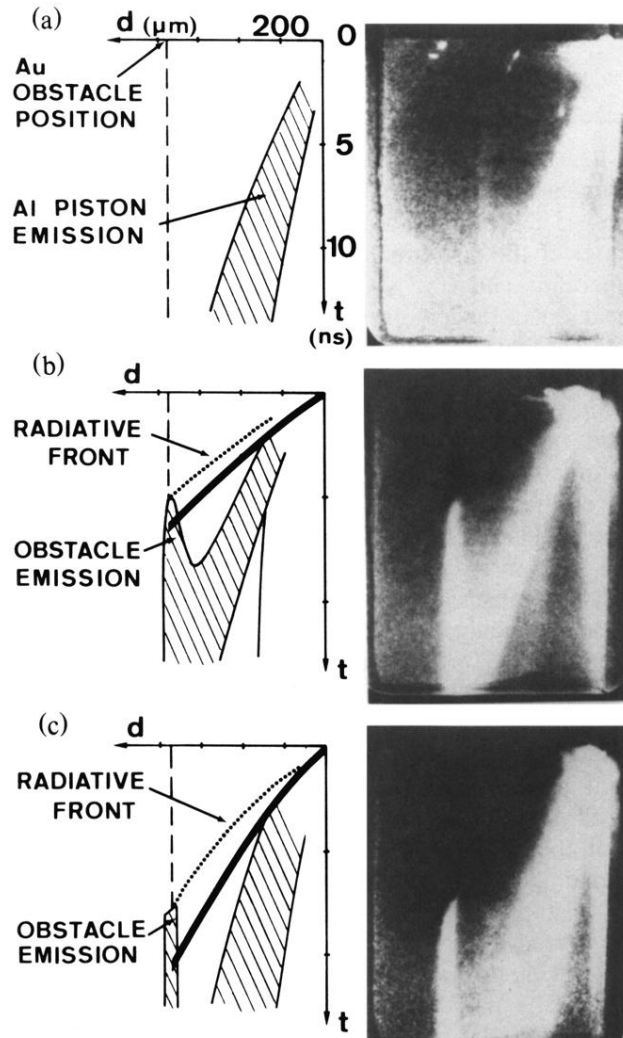


FIG. 2. Comparison between the streak photographs (hatched zones) and the results of the radiative heat conduction model (solid lines). Dotted lines represent the experimental radiative front. The 10- μm -thick Al piston moves in (a) vacuum, (b) 2 bars of xenon gas, and (c) 6 bars of xenon gas. The laser is incident from the right and the irradiance is about $4 \times 10^{14} \text{ W} \cdot \text{cm}^{-2}$.

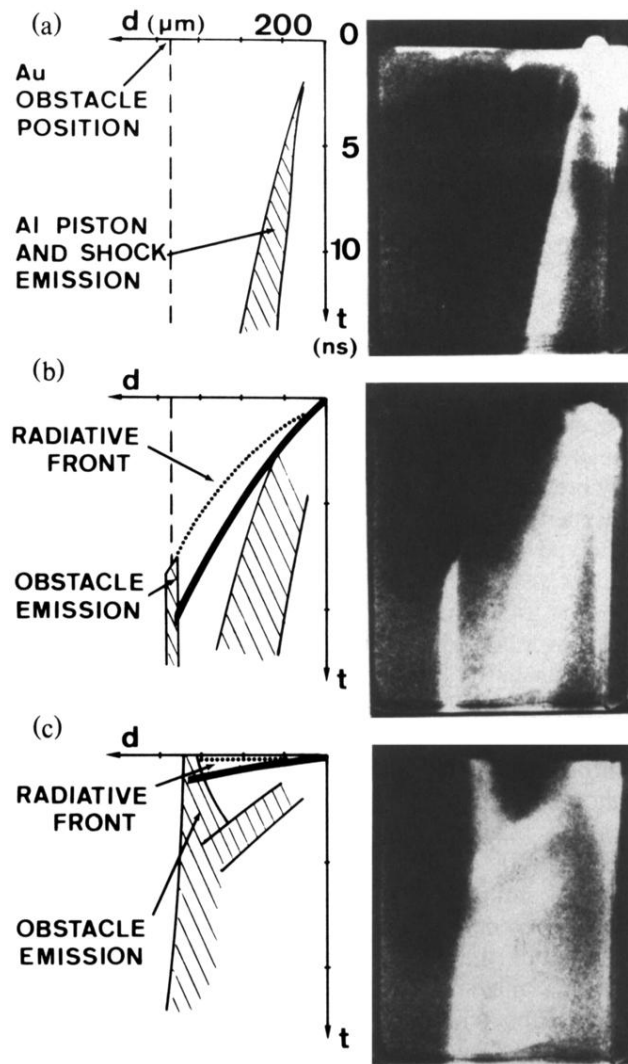


FIG. 3. Streak photographs compared to radiation-model results obtained for three different piston velocities in a shock tube filled with 6 bars of xenon. (a),(b) 2.5×10^6 and $5 \times 10^6 \text{ cm} \cdot \text{s}^{-1}$, respectively, with $1.06\text{-}\mu\text{m}$ laser light; (c) $1.2 \times 10^7 \text{ cm} \cdot \text{s}^{-1}$ with $0.35\text{-}\mu\text{m}$ laser light.